

EQUAL CHANNEL ANGULAR EXTRUSION OF HIGH PURITY GOLD

W. Yiu Yeung¹, R. Wuhler², M. Cortie³ and M. Ferry⁴

¹Department of Chemistry, Materials and Forensic Sciences, ²Microstructural Analysis Unit, ³Institute for Nanoscale Technology, University of Technology Sydney, Broadway NSW 2007 Australia

⁴School of Materials Science and Engineering, University of New South Wales, Sydney NSW 2052 Australia

ABSTRACT

Equal channel angular extrusion (ECAE) has attracted significant research interest in recent years because of its capacity to produce submicron- and nano-grained bulk materials. A high purity (99.99%) gold billet of 10 mm diameter, was processed with up to 9 repeated extrusion passes, using the ECAE technique. Mechanical properties of the extruded gold were determined by microhardness and nanoindentation measurements. It was found that the gold sample was substantially hardened after the 1st extrusion pass, with a microhardness increase from ~30 HV to ~60 HV. The hardness continued to increase with further extrusions, but at a lower hardening rate. After 9 extrusion passes, a microhardness of ~80 HV was achieved. Grain refinement of the extruded gold was assessed after the 9 extrusion passes via electron backscattered diffraction (EBSD) analysis. Results of EBSD analysis showed substantial grain refinement in the extruded metal. Grain sizes of the extruded sample were found in the range of 50 – 350 nm, with an average value of ~140 nm. A high volume of ~80% of high angled grain boundaries (>15°), was identified in the extruded material. Orientation distribution of the grains was also investigated, showing no strong textures. Development of weak {110} components was however observed.

1. INTRODUCTION

Global demand for high caratage (>22 carat) gold jewellery continues to increase. In China, Taiwan and Hong Kong, interest is traditionally focussed on 24 carat Chuk Kam jewellery, which must contain at least 99% Au for legal reasons, while in India and Arabic countries gold jewellery is normally 22 and 21 carats respectively (corresponding to 91.6 and 87.5 %Au) [1]. Such high caratage gold is extremely soft in the as-cast and annealed states. For example, 24 carat gold is about 20 HV when in the annealed state, although it can be hardened by cold work to about 80 HV. This softness means that modern jewellery designs with fine structural detail cannot be readily realized in high caratage gold alloys, and instead such items must be quite solid and 'chunky' in nature. Nevertheless, the rapid modernization and economic growth of the Asian economies means that there is a large potential market for high caratage jewellery with modern designs. Of course gold can be readily hardened by alloying, and several high caratage alloys have been developed [1], but it will be appreciated that other or complementary means to improve the strength are of great interest. For high carat gold alloys, the possibilities to harden an alloy by alloying are limited due to the small amounts of alloying elements that can be added. In addition, alloying may reduce corrosion resistance and the rich yellow colour of gold, decreasing its value.

In practice, gold is the most malleable of all metals, and can be cold worked to a foil of 50 nm or so in thickness, typically corresponding to a true strain of ~10. The flow stress of such foils is estimated [2] to be

of the order of 440 MPa, considerably greater than the ~120 - 130 MPa of annealed gold, but with reduced ductility [3]. Similarly gold can be drawn to wire of 10 µm in diameter, potentially with similar strengths. However, wire and foil have limited use in jewellery design, and a technique to produce such high strengths in gold billets would be extremely useful. In the last ten years, the development of nano- and submicron-structured materials has attracted significant research interest. An innovative technology called the Equal Channel Angular Extrusion (ECAE) process [4] has demonstrated a capability for producing nano- and submicron-structured metallic alloys, with a substantial improvement of strength. ECAE imposes a very heavy shear deformation on bulk materials without causing major dimensional changes to the extruded products. The lack of change in external dimensions differentiates it from conventional extrusion. The extrusion die is constructed with two channels of equal cross-section intersecting at a design angle. Shear deformation occurs in the material when it passes through the angular intersection connecting the two channels. The extrusion pass is repeated to increase the magnitude of strain imposed on the material. The initial structure of the material is then broken up into submicron- and nano-structures [5], and the strength and hardness of the material will substantially increase [6-8]. On the other hand ECAE research on gold alloys is very limited. In a recent study, Gubicza et al. [9] has reported grain size refinement of a high purity (99.99%) gold to ~460 - 490 nm with yield strength of about 230 MPa after 4 ECAE passes. In the present study, application of ECAE process is employed to produce high purity gold, targeting a strength up to 400 MPa

and a retained ductility to enable the production of pure gold jewellery. The grain size and strength development of the extruded gold metal will be investigated and analysed.

2. EXPERIMENTAL

A 10 mm (diameter) x 15 mm (length) 24 carat (99.99% purity) gold billet was extruded at room temperature by the ECAE process. Extrusion was conducted at a velocity of 10 mm/min. An equal channel die of 90° internal angle, which imposes to a strain of 1.15 each extrusion pass, was used in this study. The gold billet was rotated 180° between each separate pass. After 9 extrusion passes, a total strain of ~10.35 was imposed on the gold billet. Microhardness measurements were conducted on the gold billet before and after the extrusions at a load of 10g to assess its strength development. Nanoindentation tests to a maximum load of 500 mN were conducted on the billet before the extrusion and after 5 and 9 ECAE passes. An UMIS machine with a Berkovich indenter was used in the nanoindentation tests. The hardness values were computed from the loading curves using the method outlined by Oliver and Pharr [10]. Electron backscattered diffraction (EBSD) measurements were performed on the gold billet after 9 ECAE passes, to determine its grain size distribution and textural evolution. EBSD was conducted in a Zeiss Supra 55VP scanning electron microscope at 20 kV using a scanning step size of 100 nm. EBSD measurements were conducted on the cross-section of the extruded billet, which is normal to the extrusion direction. The examined area was finely polished with diamond paste and colloidal silica before examination.

3. RESULTS

3.1 Microhardness Measurements

Microhardness measurements were conducted on gold billet before and after extrusion passes. The results are plotted against total strain as shown in Figure 1. A scanning electron micrograph showing microhardness indent on the surface of extruded gold billet is presented in Figure 2. It was found that the hardness of the gold billet increased from an initial value of 30.7 HV to 62.6 HV after the first extrusion pass at a strain of 1.15, showing a substantial improvement in material strength. Hardness of the sample continued to increase with further extrusions, but the rate of hardening decreased. A hardness of 82.7 HV was achieved after 9 extrusion passes at a total strain of 10.35.

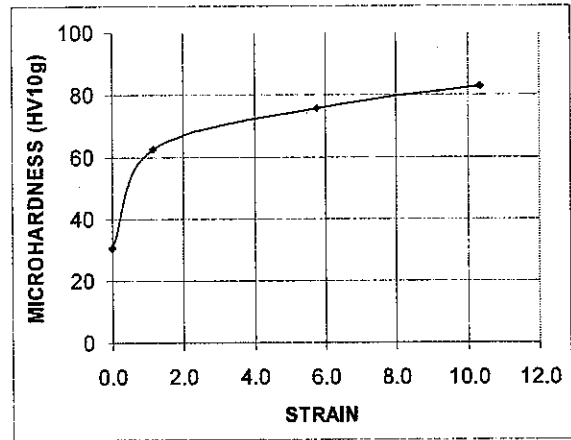


Figure 1. Microhardness of the 24 carat gold solid versus total strain of extrusion.

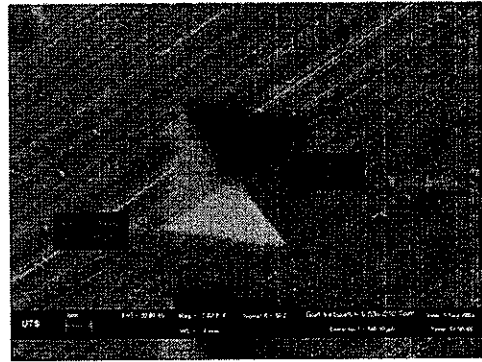


Figure 2. Scanning electron micrograph showing microhardness indent on the surface of extruded gold billet (after 5 ECAE passes).

3.2 Nanoindentation Tests

Nanoindentation tests were performed on the gold billet before extrusion and after 5 and 9 ECAE passes to a maximum load of 500 mN. The loading and unloading results of the nanoindentation tests are shown in Figure 3. A substantial hardening of the gold billet was evident after ECAE processing. It was found that at the maximum loading of 500 mN, the penetration depth of the indenter decreased from 6.54 μm of the initial material to 5.40 μm and 4.95 μm respectively after 5 and 9 ECAE passes. The hardness values were determined to be 0.5, 0.77 and 0.96 GPa for the initial material and after 5 and 9 ECAE passes respectively.

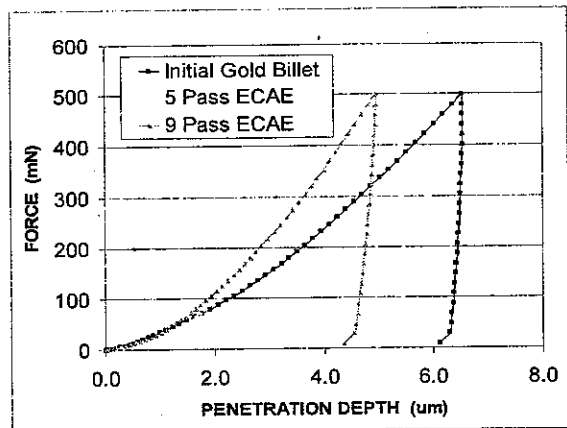


Figure 3. Nanoindentation load-displacement curves of the initial material and after 5 and 9 ECAE passes.

3.3 Electron Backscatter Diffraction Analysis

An EBSD map of the extruded sample is shown in Figure 4. Its misorientation distribution is given in Figure 5. The correlated and uncorrelated misorientations are shown in Figure 5, where a correlated misorientation displays the data between two neighbouring measurement points and an uncorrelated misorientation shows the misorientation between chosen points in the data set. The correlated data is more relevant to the present study. It was found that the extruded gold sample contained 80% of high angled grain boundaries (of misorientations $>15^\circ$), and relatively lacked of low angled grain boundaries. The grain size distribution in the extruded metal was also analysed using the data from the EBSD map. It was found that the grain size of the extruded gold was in the range of 50 nm to 350 nm with an average value of ~ 140 nm, showing establishment of an ultrafine grained structure in the extruded metal.

3.4 Texture Evolution

Texture analysis was performed on the extruded gold solid using data collected from EBSD measurements. The $\{111\}$, $\{100\}$ and $\{110\}$ pole figures of the ECAE metal are shown in Figure 6. Its inverse pole figure and orientation distribution function (ODF) are shown in Figures 7 and 8 respectively. There was no

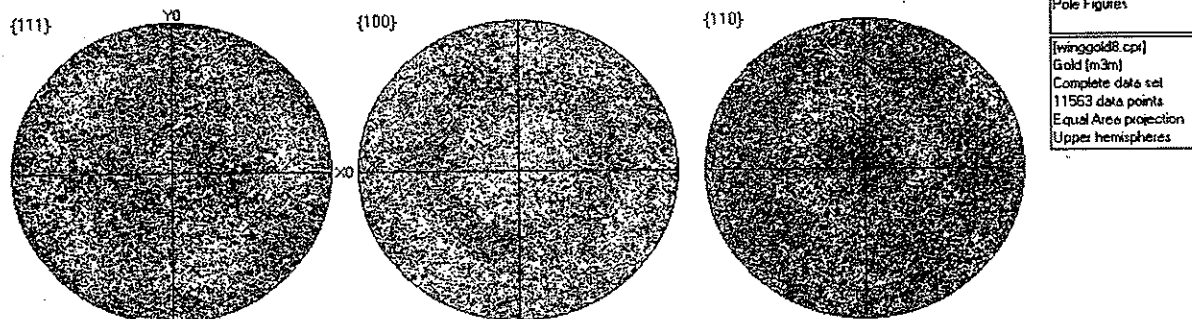


Figure 6. $\{111\}$, $\{100\}$ and $\{110\}$ pole figures of the gold billet after 9 ECAE passes.

strong texture development in the extruded metal but a weak $\{110\}$ component was identified in the metal along the extrusion direction.

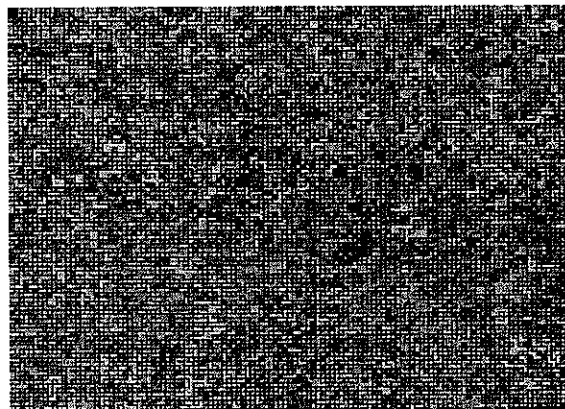


Figure 4. EBSD map of gold solid after 9 ECAE passes, high angled grain boundaries ($>15^\circ$) shown in black.

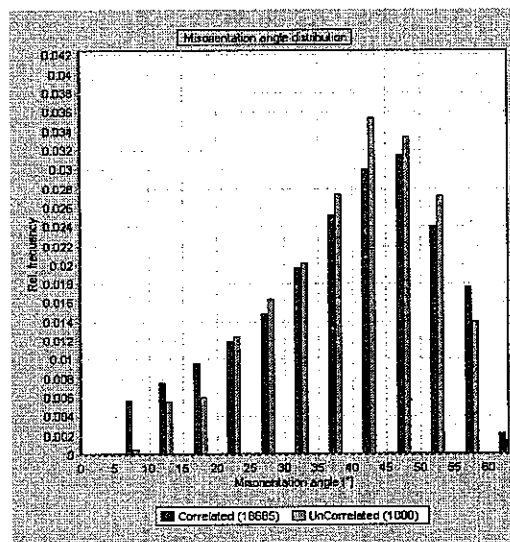


Figure 5. Misorientation distribution of grain boundaries in the extruded gold sample.

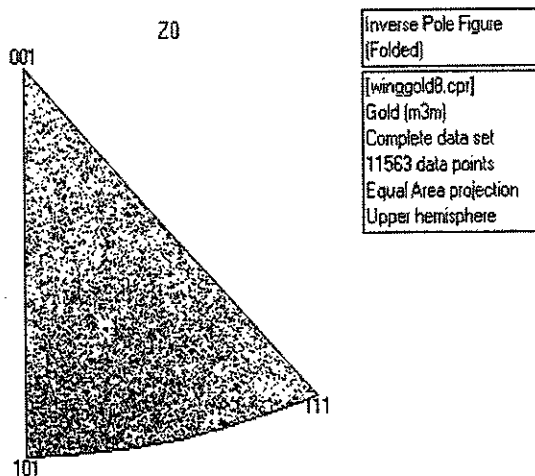


Figure 7. Inverse pole figure of the gold billet after 9 ECAE passes.

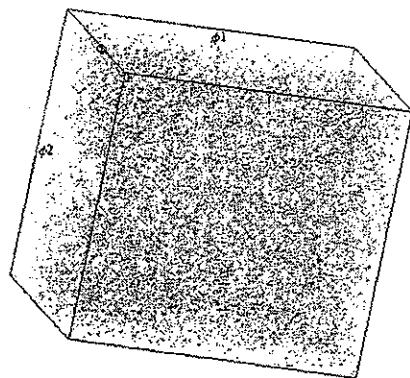


Figure 8. Orientation distribution function (ODF) of the gold billet after 9 ECAE passes.

4. DISCUSSION

Equal channel angular extrusion was applied to refine the grain structure of high purity gold in this study. It is believed that with development of an ultrafine grained structure, the gold will exhibit enhanced properties with both high strength and ductility for the production of high value pure gold jewellery. In studies of other metals, it has been reported that once an ultrafine grained structure develops, high ductility of the material could be retained after ECAE processing [11-13], that will be greatly beneficial to the subsequent metalworking of gold jewellery. In the present study, a refinement of the grain structure to ~140 nm was achieved in the gold sample after 9 ECAE passes, with a high percentage (>80%) of high angled grain boundaries (>15°). The microhardness of the processed metal was also found to increase from ~30 HV to ~80 HV. An analysis of the hardness data, shown in Figure 1, however suggested that different hardening

mechanisms might have been involved through the ECAE process. It was found that the hardness of the gold billet increased abruptly from an initial value of 30.7 HV to 62.6 HV after the first extrusion pass, showing a substantial improvement in material strength. Hardness of the gold solid continued to increase with further extrusions, but the rate of hardening was reduced. With the result obtained, an empirical equation for the hardness (H) of the gold solid vs total strain (ϵ) was established:

$$H = H_0 + A_1 (1 - e^{-\epsilon/B_1}) + A_2 (1 - e^{-\epsilon/B_2})$$

where H_0 is the initial hardness of the material, A_1 and A_2 , and B_1 and B_2 are parameters in relation to material properties and deformation strain respectively, to accommodate the different hardening effects on the material with increasing strain. In the present study, $H_0 = 30.7$ HV, $A_1 = 27.2$ HV, $A_2 = 33.4$ HV, $B_1 = 0.10$, $B_2 = 7.65$.

In an earlier study of ECAE processing of aluminium alloys, Gholinia et al. [5] reported that shear banding occurred in the early stage of deformation, and with increasing strain, high angled grain boundaries developed, leading to establishment of submicron- and nano-structures. In a recent study of ECAE processing of pure gold, Gubicza et al. [9] suggested that there were significant densities of dislocations and planar faults, and the shearing during the process was accommodated through the introduction of both dislocations in plastic deformation and planar faulting, due to the low stacking fault energy of 45 mJ m⁻² for pure gold. In the present study, the initial abrupt hardness increase of the gold is therefore likely to be associated with work-hardening of the material through the shearing deformation of the ECAE process. Work-hardening generally reduces the ductility of the material. On the other hand, with an increasing number of extrusion passes, an ultrafine grained structure was eventually established as observed, hardness of the gold solid continued to increase but at a reduced hardening rate. It is believed that this second stage of hardness development is attributed to the grain refinement in the gold sample through the ECAE processing.

In conventional materials, according to the Hall-Petch relationship, as the grain size of a material decreases, the strength and hardness of the material will substantially increase [14,15]. The derivation of this relationship relies on the stress concentration acting on a grain boundary due to a pile-up of dislocations in the first grain. However there are fundamental problems with extrapolating this model to nanostructured materials. It will become difficult to create a pile-up of dislocations in the very small grains. While Gubicza et al. [9] mentions the yield strength of pure gold of 460 – 490 nm of their study can be incorporated into a modified Hall-Petch relationship, it should be noted that different deformation behaviours, namely grain boundary/subgrain boundary/non-basal slip activities

versus conventional dislocation mechanisms have been suggested in other studies [16-20] in controlling the mechanical properties of some nanostructured materials. Mechanical behaviour of the nanostructured pure gold processed in this study is being further investigated.

5. CONCLUSION

High purity (99.99%) gold was processed by equal channel angular extrusion. Hardness of the gold sample was found to increase from 30.7 HV to 82.7 HV after 9 ECAE passes. A two-stage hardening behaviour was evident. Electron backscatter diffraction showed that significant grain refinement was achieved through the ECAE processing, with an average grain size of ~140 nm in the extruded metal. A high volume of ~80% of high angled boundaries ($>15^\circ$) was identified in the extruded gold solid. Orientation distribution of grains was analysed, showing no strong texture development, however a weak $\{110\}$ component was identified in the metal along the extruded direction.

Acknowledgements

The authors are grateful to Mr. Nanang Purhan and Dr. Yu Wang of the University of New South Wales, Australia for their assistance in equal channel angular extrusions and nanoindentation tests. The authors would also like to thank Darren Attard from ANSTO for advice with sample preparation.

References

1. C. W. Corti, *Gold Bulletin*, vol. 32 (1999) 39.
2. J. Nutting & J. L. Nuttal, *Gold Bulletin*, vol. 10 (1977) 2.
3. J. G. Cohn, *Gold Bulletin*, vol. 12 (1979) 21.
4. R.Z. Valiev, N.A. Krasilnikov and N.K. Tsenev, *Mater. Sci. Eng.*, vol. A137 (1991) 35.
5. A. Gholinia, J.R. Bowen, P.B. Prangnell and F.J. Humphreys, *Proc. 6th Int. Conf. on Aluminium Alloys*, vol. 1 (1998) 577.
6. R.W. Siegel, *Nanostr. Mater.*, vol. 4 (1994), 121.
7. Y. Wang, M. Chen, F. Zhou and E. Ma, *Nature*, vol. 419 (2002), 912.
8. E. Meijer, N. Armstrong and W.Y. Yeung, *Solid State Phenomena*, vol. 118 (2006) 53.
9. J. Gubicza, N. Q. Chinh, P. Szommer, A. Vinogradov & T. G. Langdon, *Scripta Mater.*, vol. 56 (2007) 947.
10. W.C. Oliver and G.M. Pharr, *J. Mater. Res.*, vol. 7 (1992) 1564.
11. A. Bussiba, A. Ben Artzy, A. Shtechman, S. Ifergan and M. Kupiec, *Mater. Sci. Eng.*, vol. A302 (2001) 56.
12. T. Mukai, M. Yamanoi, H. Watanabe and K. Higashi, *Scripta Mater.*, vol. 45 (2001) 89.
13. I. Nikulin, R. Kaibyshev and T. Sakai, *Mater. Sci. Eng.*, vol. A407 (2005) 62.
14. E.O. Hall, *Proc. Phys. Soc. (Lond.)*, vol. B64 (1951) 747.
15. N. J. Petch, *J. Iron Steel Inst.*, vol. 174 (1953) 25.
16. T.G. Nieh and J. Wadsworth, *Scripta Metall. Mater.*, vol. 25 (1991) 955.
17. R.O. Scattergood and C.C. Koch, *Scripta Metall. Mater.*, vol. 27 (1992) 1195.
18. N. Wang, Z. Wang, K.T. Aust and U. Erb, *Acta Metall. Mater.*, vol. 43 (1995) 519.
19. J. Koike, T. Kobayashi, T. Mukai, H. Watanabe, M. Suzuki, K. Maruyama and K. Higashi, *Acta Mater.*, vol. 51 (2003) 2055.
20. F.H. Dalla Torre, E.V. Pereloma and C.H.J. Davies, *Acta Mater.*, vol. 54 (2006) 1135.